Optical Engineering

OpticalEngineering.SPIEDigitalLibrary.org

Geometrical effect characterization of femtosecond-laser manufactured glass microfluidic chips based on optical manipulation of submicroparticles

Domna G. Kotsifaki
Mark D. Mackenzie
Georgia Polydefki
Ajoy K. Kar
Mersini Makropoulou
Alexandros A. Serafetinides

SPIE.

Domna G. Kotsifaki, Mark D. Mackenzie, Georgia Polydefki, Ajoy K. Kar, Mersini Makropoulou, Alexandros A. Serafetinides, "Geometrical effect characterization of femtosecond-laser manufactured glass microfluidic chips based on optical manipulation of submicroparticles," *Opt. Eng.* **56**(12), 124111 (2017), doi: 10.1117/1.OE.56.12.124111.

Geometrical effect characterization of femtosecond-laser manufactured glass microfluidic chips based on optical manipulation of submicroparticles

Domna G. Kotsifaki,[a,*] Mark D. Mackenzie,[b] Georgia Polydefki,[a] Ajoy K. Kar,[b] Mersini Makropoulou,[a] and Alexandros A. Serafetinides[a]
[a]National Technical University of Athens, Physics Department, Laboratory of Optoelectronics, Lasers and their Applications, Athens, Greece
[b]Heriot-Watt University, Institute of Photonics and Quantum Sciences, School of Engineering and Physical Sciences, Non-Linear Optics Group, Edinburgh, United Kingdom

Abstract. Microfluidic devices provide a platform with wide ranging applications from environmental monitoring to disease diagnosis. They offer substantive advantages but are often not optimized or designed to be used by nonexpert researchers. Microchannels of a microanalysis platform and their geometrical characterization are of eminent importance when designing such devices. We present a method that is used to optimize each microchannel within a device using high-throughput particle manipulation. For this purpose, glass-based microfluidic devices, with three-dimensional channel networks of several geometrical sizes, were fabricated by employing laser fabrication techniques. The effect of channel geometry was investigated by employing an optical tweezer. The optical trapping force depends on the flow velocity that is associated with the dimensions of the microchannel. We observe a linear dependence of the trapping efficiency and of the fluid flow velocity, with the channel dimensions. We determined that the highest trapping efficiency was achieved for microchannels with aspect ratio equal to one. Numerical simulation validated the impact of the device design dimensions on the trapping efficiency. This investigation indicates that the geometrical characteristics, the flow velocity, and trapping efficiency are crucial and should be considered when fabricating microfluidic devices for cell studies. [DOI: 10.1117/1.OE.56.12.124111]

Keywords: femtosecond laser; microfluidics; optical tweezers; glasses; geometrical characteristics; velocity measurements.

Paper 171689 received Oct. 26, 2017; accepted for publication Dec. 4, 2017; published online Dec. 27, 2017.

1 Introduction

Efforts to develop miniaturized instrumentation for medical analytical platforms have steadily increased in recent years. Microfabricated devices, which are relatively inexpensive and easy to fabricate, have proven to be useful analytical tools for a diverse range of pharmacy, biology, and tissue engineering experiments.[1] Regularly, microfluidic devices are developed by photolithography[2] and include techniques such as wet etching, cutting, and embossing. Such methodologies can create complex devices with dimensions of channels ranging from 10 to 500 μm. Various polymers have been used to fabricate microfluidic devices, due to numerous advantages coming from their intrinsic properties, but they suffer from some significant drawbacks making them unsuitable to certain applications.[2] One major restriction, especially in biology experiments, is their affinity with small hydrophobic biomolecules, such as proteins and drugs, which can lead to biomolecular absorption from solution.[2] Moreover, its permeability to water vapor leads to the evaporation from inside the microfluidic channels.[3] Furthermore, the robustness and suitability of polydimethylsiloxane (PDMS) devices for long-term use, especially in field-usable prototypes, remain questionable.[2,3] Glass-based microfluidic devices, which initially came out of the microelectronics industry, have excellent biocompatibility. However, glass substrate is becoming largely overshadowed by the use of polymer due to the technically challenging method of creating the channels. With the rapid development of ultrashort pulse technology, many researchers have investigated the fabrication of microfluidic channels by employing femtosecond-laser pulses. Femtosecond-laser direct writing[4–10] is a unique micromachining tool that allows the high-precision modification of the surface or the bulk of a transparent material, producing three-dimensional (3-D)-localized components.

In the realm of single-cell analysis, it is crucial to obtain appropriate sufficient number of cells for statistical analysis.[11] Conventional techniques for single-cell analysis include well-established methods, such as flow cytometry or fluorescence-activated cell sorting, which can detect, sort, and collect cells with desired properties. However, these techniques are based on intrinsic physical characteristics of the particles, including size, shape, and deformability, which limit the desired sensitivity, precision, high-throughput, and the low-cost.[11] As an alternative, microfluidics can meet the needs to isolate or trap single cells from high number density cell populations with high-throughput processing. To design and develop microfluidic devices, it is necessary to correlate the geometric characteristics of the microchannel with the micromanipulation of the particle. Factors impacted by the specific geometric microfluidic characteristics include the ability to isolate large numbers of cells or particles, with

*Address all correspondence to: Domna G. Kotsifaki, E-mail: dkotsifaki14@gmail.com, dkotsifaki@central.ntua.gr

0091-3286/2017/$25.00 © 2017 SPIE

high accuracy, and the fluid forces generated during fast trapping. Other properties that may affect the trapping efficiency are any geometrical variability due to small-scale microfabrication inconsistencies, the microfluidic inlet, outlet, width, height, and length of each channel, and the input concentration of the cell/particle suspension.

In this work, the microfluidic devices were fabricated by femtosecond irradiation of glass substrates with subsequent etching in diluted hydrofluoric (HF) acid. This simple and cost-effective method allows the fabrication of 3-D microfluidic devices of several geometries with much greater ease as compared to other techniques, such as multilayer soft lithography using polymers. After fabrication, we investigated the impact of various geometric characteristics of microfluidic channel on the trapping efficiency of single particle capture in a stable velocity regime. We noticed that the trapping efficiency and, therefore, the fluid drag force have a linear dependency on the dimensions of the channel. We observed that microfluidic devices, for which the ratio between the channel width and the channel height lies close to unity, trap nanoparticles with the maximum trapping efficiency and those for which the ratio is below unity, the trap was weaker. Numerical simulations confirmed that the calculated geometry dimensions permitted partitioned flow between the main microchannel and the different dimensional parameter channel and that the interaction of the fluid with the different geometries can produce areas of low or high flow velocity. In this investigation, we demonstrated that the geometry parameters of microfluidic devices are essential, impacting on flow within the device and trapping within the channels and should be well considered in fabricating microfluidic devices especially for medical or biological studies, to maximize performance.

2 Device Fabrication and Implementation

2.1 *Fabrication of Microfluidic Chips*

Microfluidic devices were fabricated in fused silica glass by irradiating with a femtosecond laser and etching with HF.[6] Figures 1(a)–1(b) show microscopic images of the microfluidic device after etching. A μ-Jewel femtosecond laser at 1047-nm wavelength (IMRA Inc.), repetition rate of 500 kHz, pulse length of 360 fs, and maximum laser power of 300 mW was focused onto the fused silica substrates that were mounted on an Aerotech XYZ stage, through 0.4 or 0.6 NA objective lenses[5] for the fabrication of the devices.

Channel width was controlled by writing varying numbers of parallel scans and channel height by varying inscription power. After writing microfluidic devices was completed, the modified material was etched for ~20 h in 5% HF solution. Tubing, with outer and inner diameter of 360 and 100 μm, respectively, was bonded to the inlets using UV curing glue. The inlets of each microfluidic device were offset vertically from the central channels and were connected by angled channels, as shown in Fig. 1(b). In this way, the imaging region moves closer to the surface of the devices, according to the working distances of the objective lens.[5] The glass microfluidic devices consist of a series of parallel horizontal channels, with a width range of 3.7 to 27 μm and a height range of 18 to 37 μm. Particular attention was given to the cross-section size of each microfluidic channel [width (w) × height (h)] to reduce the interference of the trapping laser beam from the microfluidic channel boundaries. Thus, the minimum effective cross-sectional size was obtained for the device with 3.7 μm × 16.1 μm dimensions.

2.2 *Experimental Procedures*

After the fabrication process, the glass microfluidic devices were characterized by measuring the optical forces exerted on polystyrene nanoparticles in flow. Specifically, we measured the trapping efficiency in microfluidic channels of various widths and several heights. The simple operation of the microfluidic device allows for an efficient and automated method for manipulation of the nanoparticles without the need for a complex optical trapping system. In brief, a continuous wave, vertically polarized Nd:YAG laser operating at 1064 nm, in TEM_{00} mode, with a maximum output power of 500 mW was used to create the optical trap at the focal point

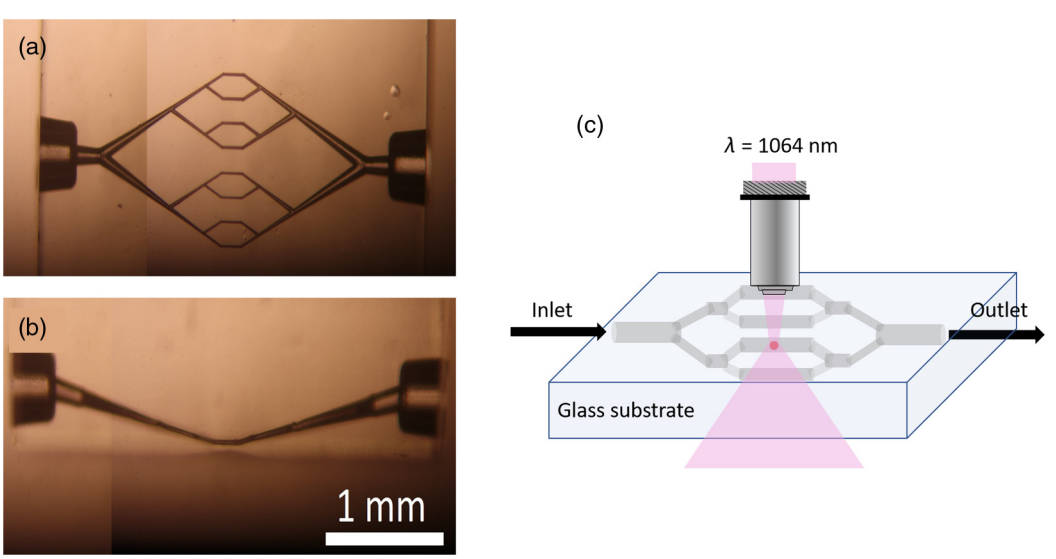

Fig. 1 Glass microfluidic device after etching: microscope images of the (a) top view of the individual microfluidic channels with width 22.6 ± 2.0 μm and height of 30.4 ± 5.0 μm and (b) side view of the microfluidic device showing that the channel moving up to the surface of the substrate. (c) Schematic of the optical trapping setup.

of a conventional optical microscope, equipped with the necessary dichroic mirror and the optical filter for the specific laser wavelength. A 100× oil-immersion objective with NA of 1.25 focuses the laser beam in the field of view, as shown in Fig. 1(c). For the optical trapping experiments, polystyrene particles with diameter of 900 nm were used, which were suspended into deionized water and sonicated before the injection into the microfluidic channel. The concentration of the nanoparticles was kept constant at 5×10^7 particle/ml. Using a syringe pump, a suspension of the nanoparticles was flown through the glass microfluidic channels. The microfluidic devices were mounted on an x-y motorized translation stage. The trapping laser propagates along z-axis. The trapping processing was monitored through a CCD camera connected to a PC. We measured the optical forces exerted on trapped nanosized particles by performing escape velocity measurements. By translating the device, at a constant velocity, under the focal point of the trapping laser beam, we measured the velocity for which the nanoparticle cannot be trapped by the laser beam for a given laser power and we determined the optical forces by Stokes law.[12] Knowing the trapping force, F, we can calculate the trapping efficiency, Q, according to the following equation:[12]

$$Q = \frac{F \cdot c}{n_{\text{med}} \cdot P}, \tag{1}$$

where P is the trapping laser power, c is the speed of light, and n_{med} is the refractive index of the surrounding medium ($n_{\text{med}} = 1.33$). The interplay between the optical trapping force and the fluid drag force determines the first criterion for the operation of the microfluidic device as a biological platform. Specifically, the channel geometrical parameters influence the flow velocity inside the microfluidic channel, thus, if the velocity of the particle is too large, then for a given laser power and objective lens there is not enough optical force to immobilize the particles.

3 Results and Discussion

Figure 2(a) shows the trapping efficiency as a function of microfluidic channel width, w, when the channel height, h, along the z-direction is kept almost constant and as a function of channel height, h, when the channel width, w, is kept constant. The results show clearly that the trapping efficiency depends strongly on the microfluidic channel dimensions. We observe that as the channel width values, w, increase the trapping efficiency decreases. The solid lines in Fig. 2(a) are linear fit to the data according to the following equations:

$$Q = Q_o + A_1 \cdot w \tag{2}$$

and

$$Q = Q_o + A_2 \cdot h, \tag{3}$$

where $Q_o = (1.45 \pm 0.11) \times 10^{-4}$ is the trapping efficiency value outside the microfluidic channel and A_1, A_2 are the fitting parameters.

To explain the relation between the trapping efficiency and the microfluidic channel width, we consider the interplay between the trapping force, Stoke's law as well as the volumetric flow rate. From Eq. (1), the trapping efficiency is based on the slope of the optical trapping forces versus laser trapping power. The optical force scales linearly with laser trapping power.[12] The Stokes' drag force scales linearly with flow rate.[13] The volumetric flow rate for the steady-state pressure-driven fluid flow in the microfluidic channel scales with the width value, according to the Hagen–Poiseuille's law.[14] Therefore, it is expected that the trapping efficiency will scale with the microfluidic channel dimensions, as found in the experiments. The maximum trapping efficiency value we obtain in this study is $Q_{\max} = (1.76 \pm 0.13) \times 10^{-4}$ at the microfluidic channel width value $w = 18$ μm. Additionally, we observe that the trapping efficiency decreases considerably as the height of the microfluidic channel is increased. A plausible explanation for the optical trapping efficiency decrease is, as the height of the microfluidic channel increases, the volumetric flow rate decreases, and therefore, the velocity of the nanoparticle and the optical trapping force decrease. Furthermore, we observe that with the microfluidic channel with 17 μm × 18 μm cross section, we obtained the highest trapping efficiency value among all.

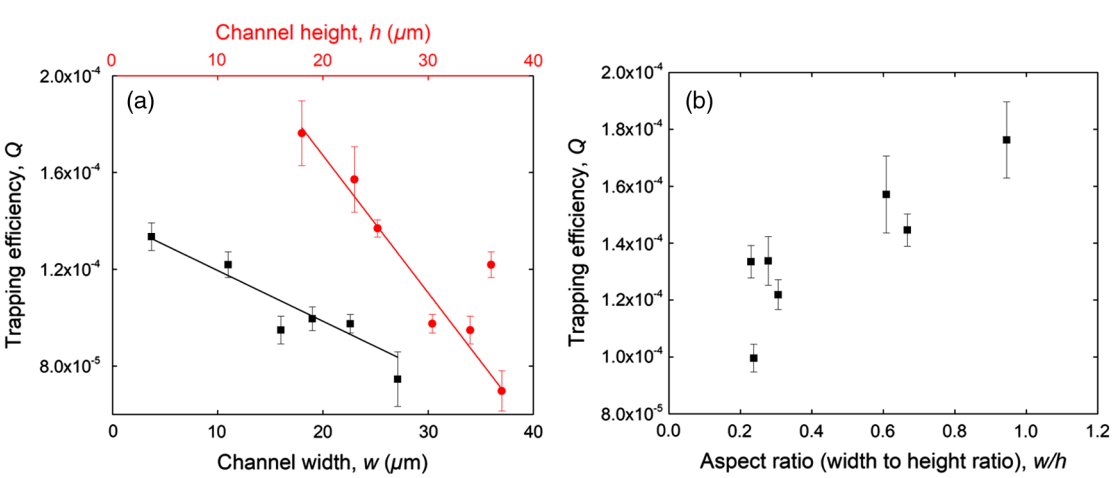

Fig. 2 (a) Trapping efficiency as a function of the microfluidic channel width (black square symbols) and as a function of the microfluidic channel height (red cycle symbols). Solid line: linear fit to the data obtained with varying microfluidic channel width values. (b) Trapping efficiency as a function of the aspect ratio (microfluidic channel width to microfluidic channel height ratio, w/h). Solid line: linear fit to the data obtained with varying microfluidic channel height values. The y-error to the standard deviation of the trapping efficiency measurements.

A corollary of the above results demonstrates that a small cross-sectional sized microfluidic channel can effectively "focus"' nanoparticles to the trapping region and, therefore, increase the efficiency of the optical trapping. Certainly, one should take into account, when designing the microfluidic channels, that the wall effect contribution and the resulting dimensionless C_DR number are influenced by the dimensions of the channel, as described in Ref. 15. In their study, the C_DR increase slightly (from 25.6 to 26.8, i.e., by ~1.2) when the separation between the cover and slide glass is reduced almost to the half (from 63 to 33 μm).[15] In our case, the variation of the cross-dimensional section of our microfluidics channels is from ~5 to 40 μm. Thus, the maximum expected C_DR increase would be no more than $3 \times \sim 1.2 = 3.6$ having a small but not negligible influence due to wall effect contribution on our trapping efficiency values.

Additionally, we investigated the influence of trapping efficiency to the material that is used for the fabrication of microfluidic devices. Thus, we designed and fabricated a simple microfluidic channel with cross-section size $100\ \mu\text{m} \times 100\ \mu\text{m}$ based on soft lithography technique using PDMS. The trapping efficiency value we obtain in this study is $Q = (1.76 \pm 0.57) \times 10^{-6}$ at the PDMS microfluidic channel, whereas the value for the glass channel is $Q = (4.51 \pm 0.89) \times 10^{-5}$ with the same geometrical dimensions, using the same experimental processing. We observed that the trapping efficiency for the PDMS channel is roughly 20 times lower than that for the glass channel. A possible explanation of the above discrepancy in the trapping efficiency values is due the elastic deformation of the PDMS, which affects the laminar flow profile. Thus, the pressure inside the PDMS microfluidic channel increases and may influence the experimental performance.

The channel aspect ratio is an important parameter in controlling the microfluidic flow in any microfluidic device. It has been reported that if the microchannel aspect ratio (microfluidic channel height divided by width, h/w) increases, the speed of liquid in the meniscus shape channel also increases.[16] To obtain a reliable result, we investigate the trapping efficiency versus the aspect ratio (channel width to channel height ratio, w/h), as shown in Fig. 2(b). We observe that the trapping efficiency increases for aspect ratio values lower than one. Moreover, the maximum optical efficiency is obtained for aspect ratio around unity. A plausible explanation for this behavior is due to the lower friction constant in the channel of low aspect ratio value, which results in a faster microfluidic flow[17] and consequently in increased trapping efficiency values. Another important factor that will influence the flow behavior is the quality of the microfluidic channel surface. This factor is beyond the scope of this paper and it will be the subject of a future investigation. Additionally, with an increase of both, the ratio of wall surface to flow volume and the ratio of microfluidic channel length to cross section, the resistance to flow in a microfluidic channel becomes high, thus requiring high pressure to drive the flow through the device.[18] This behavior of the microfluidic channels tends to have a high resistance to flow, resulting in low-flow velocities and therefore low trapping efficiency values. The above analysis implies that the optical trapping processing in a microfluidic device can be further improved by decreasing the cross section of the channel, provided that the small channel can be appropriately fabricated to minimize the interactions between the particles and the channel walls.

A model of fluid flowing in the channel of the microfluidic device was developed to understand how channel dimensions will affect the flow velocity and thereby the trapping efficiency. Thus, COMSOL multiphysics simulation was performed in 3-D to simulate the laminar fluid flow in the glass microfluidic channel. The Newtonian fluid dynamic module solved the Navier–Stokes equation at steady state.[14] The density and viscosity values were specified for water at room temperature (25°C, the density of the water was $998.2\ \text{kg/m}^3$ and the dynamic viscosity of water was 1.003×10^{-3} Pa s). Microfluidic channel layout and dimensions were taken from the glass microfluidic device design. A Poiseulle boundary condition was applied at the inlet, with a zero-pressure outlet and a no-slip fluid wall interface. These boundary conditions were imposed to solve the laminar flow. Mesh refinements were performed to minimize the flow flux between inlet and outlet.

Figure 3(a) shows the velocity field inside the glass microfluidic channel with cross-section size (i) $11\ \mu\text{m} \times 36\ \mu\text{m}$ and (ii) $14\ \mu\text{m} \times 23\ \mu\text{m}$. We observe that the velocity magnitude decrease strongly depends on channel width: the higher the channel width, the lower the velocity. Moreover, the flow velocity magnitude in the central regions of the trap is increasing as the geometrical parameters values are reducing. Additionally, we show that the geometrical dimensions permit portioned flow between the main channel and the channel where the optical trap is located. To further understand this result, we investigate the maximum velocity versus channel width and height, as shown in Fig. 3(b). We observe that our experimental behavior of the results is relatively close by those yielded by simulation for channel width and height values <15 μm. For channel dimension values, larger than 15 μm, the simulation results show the velocity values almost constant. This discrepancy maybe due to the fact that the velocity magnitude also depends on two parameters, the length of the straight channel and the bypass channel, based on the flow resistance theory. The length of the microfluidic channel of each device could not be of the same value, due to some fabrication processing restrictions and thus the above-mentioned parameters may affect the experimental results.

The velocity along the mean line of the middle microfluidic channel width, w, is shown in Fig. 3(c), for cross-section size dimensions $4\ \mu\text{m} \times 10\ \mu\text{m}$ and $10\ \mu\text{m} \times 4\ \mu\text{m}$. We obtain the microfluidic device design, depicted parabola velocity field, with a maximum velocity in the center of the channel, which is desirable for the homogeneous specimen accumulation in the channel.[19] To be more explicit, when the particle is pushed into the device, the force applied will influence the flow velocity in the microfluidic channel. If the flow velocity is higher, the number of particles in the channel and their location will change. Thus, to optimize the loading capacity with uniform particle distribution around the microfluidic channel, it is necessary to modify the channels dimensions to flatten the velocity dispersion. Moreover, we observe that as the channel width increases and the channel height decreases, for microfluidic devices with the same cross-sectional area [Fig. 3(c)], a slight shift of some submicrons (~0.465 μm) in the location of the peak velocity in

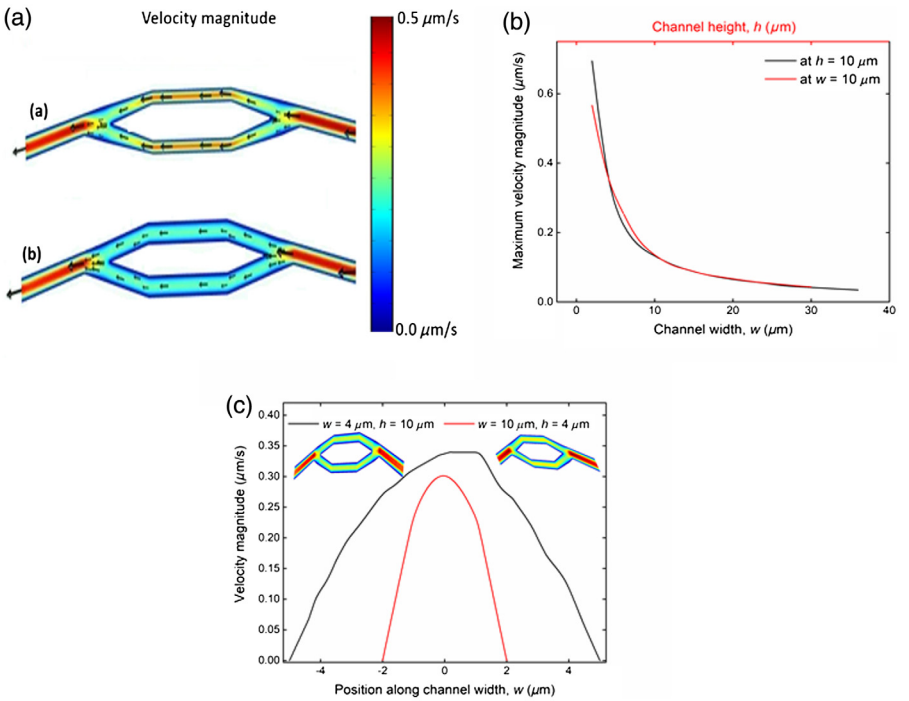

Fig. 3 (a) Numerical simulation of velocity magnitude in microfluidic channel with cross-sized section (a) 11 μm $\times$ 36 μm and (b) 14 μm $\times$ 23 μm. The arrows were used to visualize the velocity field. (b) The maximum velocity magnitude as a function of microfluidic channel width (black line) and microfluidic channel height (red line). (c) The velocity profile along the channel width is parabolic with increasing maximum velocity toward the center of the channel along the channel width. The inset illustrates the velocity magnitude profile for each cross-section size value.

the channel is established. Therefore, the experimentally obtained reduction of the trapping efficiency, due to channel width increase, is due to the peak velocity shift in the microchannel.

Recently, it was reported that the hydrodynamic forces in a laminar flow have the same order of magnitude of forces produced by optical tweezers (tens of pN),[20] based on theoretical modeling and experimental verification of the behavior of microparticles, flowing in microfluidic conduits, exposed to gravitational and lift forces and to the velocity gradient. Furthermore, as is the case of a bulk microscope-based optical tweezers, the combined system requires careful alignment, and we can foresee that the latter is not a good candidate in clinical applications by nonoptical tweezers-specialized personnel. For that reason, a combination of a fiber-based optical tweezers and microfluidic circuits, with a fully integrated approach, will be a solution for cost reduction and miniaturization, very important for point-of-care applications. In a previous work of ours, the optical trapping force and the effective trapping quality factor of a single-optical fiber trap were measured, as well as the dependence of the trapping force on both the insertion angle of the fiber into the sample chamber and the size of the trapped particle.[21] As the optical trapping forces exerted on particles in flow are affected by the geometrical characteristics of the device, there is a need to verify and calibrate the intercorrelation of both the optical and hydrodynamic forces.

4 Conclusions

Summarizing, we have utilized a noninvasive, versatile, and efficient method based on optical tweezers for the investigation of the microfluidic channel geometrical dimensions on the trapping efficiency of nanoparticles. The microfluidic devices were fabricated using ultrafast laser inscription and chemical etching of fused silica glass. We determine that the use of small cross-section channel shows maximum trapping efficiency values. It was also found that decreasing the channel height may have a more pronounced effect in increasing the trapping efficiency than decreasing the channel width. Moreover, it was observed that the aspect ratio of microfluidic channels plays an important role, both in determining the flow velocity in the microchannel where the trap is located and in enhancing of the trapping efficiency. Through numerical simulations, we confirmed that the geometrical dimensions influence the ability to perform high-throughput optical manipulation. This investigation showed that the geometrical dimensions of the microfluidic channel strongly influence its behavior and so should be optimized for each biological application using high-throughput manipulation of nanometer scale particles. This demonstration shows that how this method can be used as a powerful tool for the characterization of microfluidic devices and the importance of preforming such characterization to maximize device performance.

Acknowledgments

D.G. Kotsifaki gratefully acknowledges the funding by the IKY Fellowships of Excellence for Postgraduate Studies in Greece-Siemens Program. Mark Mackenzie acknowledges funding from the Engineering and Physical Sciences Research Council Grant No. EP/M015130/1.

References

1. A. Alrifaiy, O. A. Lindahl, and K. Ramser, "Polymer-based microfluidic devices, biology and tissue engineering," *Polymers* **4**, 1349–1398 (2012).
2. M. W. Toepke and D. J. Beebe, "PDMS absorption of small molecules and consequences in microfluidic applications," *Lab Chip* **6**, 1484–1486 (2006).
3. G. Velve-Casquillas et al., "Microfluidic tools for cell biological research," *Nano Today* **5**(1), 28–47 (2010).
4. C. Iliescu et al., "A practical guide for the fabrication of microfluidic devices using glass and silicon," *Biomicrofluidics* **6**, 016505 (2012).
5. V. K. Jagannadh et al., "Imaging flow cytometry with femtosecond laser micromachined glass microfluidic channels," *IEEE J. Sel. Top. Quantum Electron.* **21**(4), 370–375 (2015).
6. D. Choudhury, J. R. Macdonald, and A. K. Kar, "Ultrafast laser inscription: perspectives on future integrated applications," *Laser Photonics Rev.* **8**, 827–846 (2014).
7. C. Li et al., "Fabrication of three-dimensional microfluidic channels in glass by femtosecond pulses," *Opt. Commun.* **282**, 657–660 (2009).
8. M. S. Giridhar et al., "Femtosecond pulsed laser micro-machining of glass substrates with application to microfluidic devices," *Appl. Opt.* **43**, 4584–4589 (2004).
9. C. Hnatovsky et al., "Fabrication of microchannels in glass using focused femtosecond laser radiation and selective chemical etching," *Appl. Phys. A* **84**, 47–61 (2006).
10. G. Li et al., "Femtosecond laser assisted fabrication of networked semi-occlusive microfluidic channel on fused silica glass surface," *Optik* **140**, 953–958 (2017).
11. H. Yin and D. Marshall, "Microfluidics for single cell analysis," *Curr. Opin. Biotechnol.* **23**, 110–119 (2012).
12. W. H. Wright, G. J. Sonek, and M. W. Berns, "Parametric study of the forces on microspheres held by optical tweezers," *Appl. Opt.* **33**(9), 1735–1748 (1994).
13. A. Zehtabi-Oskuie, J. G. Bergeron, and R. Gordon, "Flow-dependent double-nanohole optical trapping of 20 nm polystyrene nanospheres," *Sci. Rep.* **2**, 966 (2012).
14. K. W. Oh et al., "Design of pressure driven microfluidic networks using electric circuit analogy," *Lab Chip* **12**, 515–545 (2012).
15. M. Miwa, S. Juodkazis, and H. Misawa, "Drag of a laser trapped fine particle in a microregion," *Jpn. J. Appl. Phys.* **39**, 1930–1933 (2000).
16. S. Mukhopadhyay et al., "Experimental study on capillary flow through polymer microchannel bends for microfluidic applications," *J. Micromech. Microeng.* **20**, 055018 (2010).
17. I. Papautsky et al., "Effects of rectangular microchannel aspect ratio on laminar friction constant," *Proc. SPIE* **3877**, 147–158 (1999).
18. X. Xue et al., "Analysis of fluid separation in microfluidic T-channels," *Appl. Math. Modell.* **36**, 743–755 (2012).
19. W. S. Low, N. A. Kadri, and W. A. B. bin Wan Abas, "Computational fluid dynamics modelling of microfluidic channel for dielectrophoretic BioMEMs application," *Sci. World J.* **2014**, 1–11 (2014).
20. J. Janča et al., "Relaxation of microparticles exposed to hydrodynamic forces in microfluidic conduits," *Anal. Bioanal. Chem.* **399**, 1481–1491 (2011).
21. D. G. Kotsifaki et al., "Optical manipulation of micro/nanoparticles using fiber-based optical tweezers," *J. Nanotechnol. Diagn. Treat.* **4**, 25–30 (2016).

Domna G. Kotsifaki is a research scientist working in photonics and optoelectronics as a member of the OLA group at the National Technical University of Athens (NTUA), Greece. She received her PhD in optical tweezers and micromanipulation of dielectric particles and biological samples using lasers in 2012. She is an expert on optical tweezers, plasmonics, biophysics, microfluidics, and optical fibers. She received national and international awards. She participated in national and international research projects where in two of them she was the coordinator.

Mark D. Mackenzie is a research scientist working in photonics as a member of the NLO group at Heriot Watt University. His work involves using ultrafast laser inscription (ULI) to fabricate waveguide lasers, supercontinuum sources, and microfluidic devices. He received his PhD in microfluidic devices and biological lasers for biophotonic applications from Heriot Watt University in 2017.

Georgia Polydefki received her BSc degree in applied mathematics from the University of Patras, Greece, her MSc degree in physics and its technological applications from NTUA, Greece, and she is currently working toward her PhD (October of 2017-NTUA). In MSc degree, she worked on optical trapping in combination with microfluidic flow systems, and in her BSc thesis, she worked on gradient and Hamiltonian dynamical systems.

Ajoy K. Kar has over 30 years of experience in studies of the nonlinear optical properties of materials and their applications. His current projects involve amplifiers for telecommunications, ultrafast all-optical switching in innovative optical fibers, and ULI of photonic devices. Recently, he has been applying the principles of nonlinear optics to develop innovative microfluidic devices for biophotonics applications incorporating three-dimensional optical waveguides to enable sorting, growth, maintenance, and assay of primary cells.

Mersini Makropoulou (NTUA) has more than 25 years of experience in laser–tissue and biomaterials interactions for medical and biophysical applications. Her research topics are biophysical mechanisms of the interaction of laser radiation with various biostructures, biomedical applications of lasers (diagnosis, therapy, and surgery), LIF spectroscopy, dosimetry of biomedical laser applications, mathematical modeling of laser–tissue interactions, and optical trapping of cells and nanoparticles. She has over 110 publications in international journals and in international conference proceedings.

Alexandros A. Serafetinides (NTUA) received his diploma in physics from the University of Athens, Greece, in 1973, his MSc and PhD degrees in optoelectronics and lasers from the University of Essex, United Kingdom, in 1974 and 1978, respectively. He has over 40 years of experience in optoelectronics, lasers, and applications. He published more than 300 articles in international journals and conferences and 7 textbooks. He participated in international and national research projects and has obtained national and international awards.